Privacy-Preserving Indoor Localization via Active Scene Illumination

Jinyuan Zhao Natalia Frumkin Janusz Konrad Prakash Ishwar
Department of Electrical and Computer Engineering
Boston University
{zhaojy11, nfrumkin, jkonrad, pi}@bu.edu

Abstract

Traditional camera-based indoor localization systems use visual information to resolve the position of an object or person. This approach, however, may not be acceptable in privacy-sensitive scenarios since high-resolution images may reveal room and occupant details to eavesdroppers. In this paper, we address privacy concerns by replacing cameras with a small network of extremely low resolution color sensors. To make the system robust to ambient lighting fluctuations, we modulate an array of LED light sources to actively control the illumination while recording the light received by the sensors. We quantitatively validate the performance of our localization approach through simulations and real testbed experiments. We quantify the impact of sensor noise and changes in ambient illumination on localization accuracy. Finally, we demonstrate the superior performance of localization via active illumination compared to passive illumination where LEDs produce constant light.

1. Introduction

A smart room, which can react to occupants' needs, will likely become a common occurrence in our lifetimes. With advanced sensors, processors and state-of-the-art algorithms, smart rooms are expected to save energy [3] and provide productivity, comfort and health benefits. Indoor localization of occupants is a key component of future smart-room applications that interact with occupants based on their locations.

Traditional vision-based indoor localization systems using fixed cameras [6, 17, 23, 25, 32, 36] are reliable and provide accurate location estimates. However, they are not suitable for venues where privacy is expected since videos can reveal details about occupants, their activities and the room itself [11]. Various techniques have been proposed to eliminate these privacy concerns. A popular way is to cover, replace or transform sensitive parts of camera images. This includes image cartooning globally [9] or locally, within sensitive objects [12], as well as using generative adversarial networks for image obfuscation [27] and human body and face de-identification [5]. While such methods work quite well, they are all based on post-processing and thus cannot prevent eavesdroppers from hacking directly into the camera to obtain the original images.

Therefore, indoor localization systems have been developed that do not use cameras. Some systems require occupants to wear an electronic device, such as a tag [14, 24, 26, 33], but this is intrusive and system performance can be affected by device placement [20]. Device-free localization systems, on the other hand, exploit signals that are affected by human activity, such as WLAN signals [18, 22, 35], ultra-wideband radio signals [10, 21, 34], airflow disruption [19], infrared rays [2, 13], audible sound [15], and ultrasound [28, 30]. These systems often suffer from environmental noise and signal reflections, and also may require re-calibration for each usage-scenario.

Another solution to address privacy concerns is to use extremely low resolution (eLR) sensors for they capture very limited visual information. Therefore, even if hacked, they are useless to eavesdroppers. A side benefit is reduced data communication and processing. eLR color sensors have been successfully used for activity recognition [8] and head pose estimation [7] at resolutions as low as 3×3 pixels. A network of single-pixel, time-of-flight (ToF) sensors mounted on a ceiling has been successful in occupant tracking and coarse pose estimation in both simulated and real-world experiments [16, 4]. A network of single-pixel color sensors has also been used for occupant localization in a real testbed [29], but without active scene illumination. However, such systems are expected to be highly sensitive to ambient light fluctuations. This sensitivity issue was partially addressed by Wang *et al.* for coarse-grained (as opposed to fine-grained) occupancy estimation using an array of modulated LED light sources and single-pixel color sensors [31]. Building upon this approach, we recently proposed two principled indoor localization algorithms using light transport analysis and validated their effectiveness in

MATLAB simulations, but we did not provide quantitative validation on a real testbed [37].

In this paper, we further advance privacy-preserving indoor localization by making the following contributions:

1. We provide the first quantitative real-world testbed validation of indoor localization based on active illumination with an array of modulated LED sources and single-pixel color sensors.
2. Ours is also the first work to demonstrate (*via* both simulations and on a real-world testbed) that an active illumination based indoor localization approach is quantitatively more accurate and robust to noise and ambient illumination variations than one based on passive illumination.
3. We improve our previous localization algorithm [37] by incorporating a new regularization prior in the objective function to dramatically reduce (by at least a factor of 4) the average localization error (see Table 5).
4. Our simulation models are more realistic than the idealized MATLAB model used in [37] that ignores noise and illumination changes. Our MATLAB simulations account for these non-idealities. We also provide simulation results using Unity3D which captures real-world illumination more accurately than a MATLAB model.

We note that our system can accurately estimate the centroid of an object in an indoor environment, but not other properties like shape, size, color making it privacy-friendly.

This paper is organized as follows. Section 2 introduces our localization algorithms for both illumination scenarios. Section 3 describes our experimental setup and results in simulated and real-world experiments. Section 4 discusses these results and points to future challenges.

2. Methodology

2.1. Light Reflection Model

We briefly introduce Wang *et al.*'s light reflection model [31], which forms the basis of our localization algorithms. Given the properties of light sources and light sensors in a room, this model relates sensor readings to the reflection properties of surfaces (see Fig. 1). The model is derived under the following assumptions:

1. The light sources and light sensors are mounted on the ceiling and face downwards; their areas are negligible compared to the area of the ceiling.
2. The light reflected by the floor is dominant; all the other reflected light can be ignored.
3. There is no direct light from any source to any sensor.
4. The floor and object are both Lambertian and flat (object heights can be ignored relative to the room height).

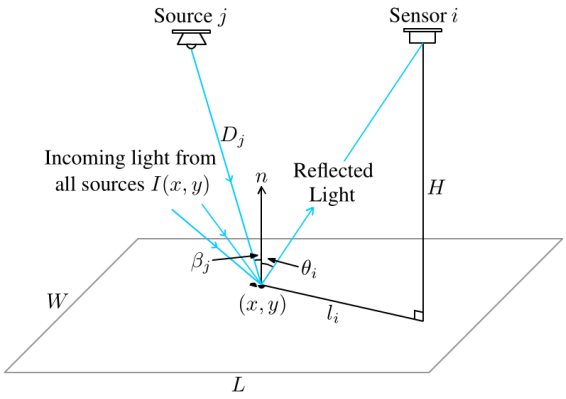

Figure 1. Light reflection model [31].

Assume that the incoming luminous (photon) flux per unit area at floor location (x, y) is $I(x, y)$. Clearly, $I(x, y)$ is the sum of luminous fluxes from all light sources:

$$I(x,y) = \sum_{j=1}^{N_f} I_j(x,y) \tag{1}$$

where $I_j(x, y)$ is the flux from source number j and N_f is the number of light sources (fixtures). For a downward-facing, point light source, we have

$$I_j(x,y) = f(j) \cdot I_{\max} \cdot q(\beta_j) \cdot \frac{\cos\beta_j}{4\pi D_j^2} \tag{2}$$

where $f(j)$ is the relative intensity of source number j scaled to lie in range $[0, 1]$, $I_{\max}$ is the maximum intensity of the light source, β_j and D_j are as shown in Fig. 1, and $q(\cdot)$ is the light intensity distribution function that describes the relative intensity of the light from the source at each angle. An example of a $q(\cdot)$ function is shown in Fig. 2.

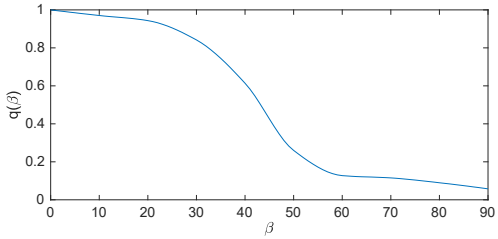

Figure 2. Example of a light intensity distribution function $q(\cdot)$.

The luminous flux captured by lensless sensor number i (i.e., sensor i's reading) is:

$$s(i) = b(i) + \int_0^W \int_0^L \frac{I(x,y)\alpha(x,y)\cos^2\theta_i}{4\pi(H^2 + l_i^2)} S dx dy \tag{3}$$

where $\alpha(x, y)$ is the floor albedo at location (x, y), S is the area of the sensor, $b(i)$ is the ambient light that arrives at sensor i, and W, L and H are the width, length and height of the room, respectively. Note that θ_i and l_i in Fig. 1 are functions of x and y.

To develop our localization algorithms, we make the simplifying assumption that the change in albedo $\Delta\alpha$ on

the floor due to the appearance of an object is a small, compact, connected region $\mathcal{P}$. Then, if $b(i)$ remains constant, the change in the reading of sensor i caused by the object appearance is:

$$\Delta s(i) = \int_{\mathcal{P}} \frac{I(x,y)\Delta\alpha(x,y)\cos^2\theta_i}{4\pi(H^2+l_i^2)} S dx dy. \quad (4)$$

We consider two types of room illumination: passive and active. A passive illumination system collects data from the scene under fixed light emitted by all light sources. The system has no control over light sources. By contrast, an active illumination system can modulate each light source at a desired frequency[1] while simultaneously collecting data from the sensors. By analyzing the light transported from each source to each sensor we can estimate an object's location on the floor due to albedo change. For each sensing method, we propose a model-based algorithm to localize a single object. Both of our algorithms localize the *change* between the current state (e.g., room occupied by an object) and an initial state (e.g., empty room) and therefore require one set of measurements for each state.

We note that our modeling assumptions, stated at the beginning of this section, are used only to *derive* our localization algorithms. They may not hold exactly in practice and indeed they do not in our physical testbed. Still, as we will see, our active localization algorithm performs consistently very well in our testbed indicating its robustness to deviations from the stated assumptions. Our empirical results validate the practical utility of our modeling assumptions despite their imperfections, which are acknowledged and discussed in Section 4.

2.2. Localization via Passive Illumination

In order to develop a localization algorithm based on passive illumination, we make the following assumptions in addition to those listed in Section 2.1:

1. The intensities of all light sources and ambient light are the same in the empty and occupied room states.
2. The object size is negligible compared to the floor size.

Under the above assumptions, the integral in (4) reduces to:

$$\Delta s(i) = \frac{I(x_0,y_0)\Delta\alpha(x_0,y_0)\cos^2\theta_i}{4\pi(H^2+l_i^2(x_0,y_0))} \cdot S \cdot S_0 \quad (5)$$

where (x_0, y_0) is the location of object's center, S_0 is the area of region $\mathcal{P}$, and $S_0 \ll W \times L$. For sensors number i_1 and i_2, the ratio of the captured changes δs is

$$\frac{\Delta s(i_1)}{\Delta s(i_2)} = \frac{(H^2+l_{i_2}^2)\cos^2\theta_{i_1}}{(H^2+l_{i_1}^2)\cos^2\theta_{i_2}} = \frac{(H^2+l_{i_2}^2)^2}{(H^2+l_{i_1}^2)^2} \quad (6)$$

[1] In practice, the modulation frequency needs to be high enough to avoid the perception of flicker by occupants.

so that the relationship between l_{i_1} and l_{i_2} simplifies to:

$$\frac{H^2+l_{i_1}^2}{H^2+l_{i_2}^2} = \sqrt{\frac{\Delta s(i_2)}{\Delta s(i_1)}} \quad (7)$$

If we substitute the coordinates of both sensors and (x_0, y_0) into equation (7) to replace l_{i_1} and l_{i_2}, then it can be re-written as a quadratic equation in x_0 and y_0:

$$a_{i_1i_2}x_0^2 + b_{i_1i_2}x_0 + c_{i_1i_2}y_0^2 + d_{i_1i_2}y_0 = u_{i_1i_2} \quad (8)$$

where $a_{i_1i_2}$, $b_{i_1i_2}$, $c_{i_1i_2}$, $d_{i_1i_2}$ and $u_{i_1i_2}$ are coefficients derived from equation (7) that depend on sensor coordinates.

In a room with N_s sensors, we can write $N_s - 1$ non-redundant quadratic equations corresponding to the sensor pairs $(i_1, i_2) = (1,2), (1,3), \ldots, (1, N_s)$. Collecting coefficients from equations (8) for all sensor pairs as follows:

$$M = \begin{bmatrix} a_{12} & b_{12} & c_{12} & d_{12} \\ a_{13} & b_{13} & c_{13} & d_{13} \\ \vdots & \vdots & \vdots & \vdots \\ a_{1N_s} & b_{1N_s} & c_{1N_s} & d_{1N_s} \end{bmatrix}, \ \mathbf{u} = \begin{bmatrix} u_{12} \\ u_{13} \\ \vdots \\ u_{1N_s} \end{bmatrix}. \quad (9)$$

we can find the object location (x_0, y_0), that is encoded in vector $\mathbf{v} = [x_0^2, x_0, y_0^2, y_0]^T$, by solving $M\mathbf{v} = \mathbf{u}$. Since this set of equations may not be satisfied exactly due to noise and modeling imperfections, we apply constrained least-squares minimization to find $\mathbf{v}$ as follows:

$$\arg\min_{\mathbf{v}} \|M\mathbf{v} - \mathbf{u}\|_{l_2}^2 \ \text{ s.t. } \mathbf{v} \geq 0, \mathbf{v} \leq [W^2, W, L^2, L]^T. \quad (10)$$

The 2-nd and 4-th entries of the solution vector, provide an estimate of the object location $(\widehat{x}_0, \widehat{y}_0)$. The cost function is strictly convex and has unique global minimum when matrix M has full column rank ($N_s \geq 5$). The pseudo-code for this algorithm appears in Algorithm 1.

Algorithm 1: Localization via Passive Illumination

Input : Vectors of sensor readings: $\mathbf{s}_0$ for empty room and $\mathbf{s}$ for occupied room, room dimensions W, L and H, sensor coordinates (x_i, y_i, H) for $i = 1, \ldots, N_s$

Output: Estimated location $(\widehat{x}_0, \widehat{y}_0)$

1 Let $\Delta\mathbf{s} \leftarrow \mathbf{s} - \mathbf{s}_0$;
2 Calculate coefficients $a_{i_1i_2}, b_{i_1i_2}, c_{i_1i_2}, d_{i_1i_2}, u_{i_1i_2}$ for $(i_1, i_2) = (1,2), (1,3), \ldots, (1, N_s)$ in (8);
3 Construct matrix M and vector $\mathbf{u}$ as in (9);
4 Use quadratic programming to find the optimal solution $\mathbf{v}^*$ to minimization (10);
5 Estimated location: $(\widehat{x}_0, \widehat{y}_0) \leftarrow (v_2^*, v_4^*)$.

2.3. Localization via Active Illumination

Using the light reflection model from Section 2.1 (with no additional assumptions), we derive our localization algorithm based on active illumination. This algorithm is a refinement of our previous localized ridge regression algorithm [37].

Let $\mathbf{s}$ be an $N_s \times 1$ vector of sensor readings, $\mathbf{f}$ an $N_f \times 1$ vector of relative source intensities, and $\mathbf{b}$ a vector of ambient light levels at each sensor. We know from equations (1–3), that the relationship between $\mathbf{s}$ and $\mathbf{f}$ is linear:

$$\mathbf{s} = A\mathbf{f} + \mathbf{b} \tag{11}$$

where A is the $N_s \times N_f$ light transport matrix [31]. The light transport matrix describes the relationship between every light source and every sensor. It is clear from equation (3) that matrix A is determined by room geometry, material properties and source and sensor locations, but it is not affected by ambient light. To estimate A, one can add a set of linearly independent perturbations $\Delta\mathbf{f}$ to any base light $\mathbf{f}_0$, measure the corresponding changes $\Delta\mathbf{s}$ from the sensors, and then solve for A [31]. We assume that the change in ambient light $\mathbf{b}$ over the duration of one set of measurements is small enough that it can be treated as constant over that duration.

Suppose that we obtain two light transport matrices, A_0 for the initial (empty room) state and A for the current state, and compute their difference $E = A - A_0$. Then, by the light reflection model (3), we can write:

$$E(i,j) = \int_0^W \int_0^L C(i,j;x,y)\Delta\alpha(x,y)\,dxdy \tag{12}$$

where $C(i,j;x,y)$ is the unit contribution of source j to the reading of sensor i *via* location (x,y). If we discretize the floor plan on a grid with spacing δ, then we can re-write the discretized approximation to this equation in matrix form:

$$\mathbf{e} = \delta^2 C\Delta\boldsymbol{\alpha}, \tag{13}$$

where vector $\mathbf{e}$ contains lexicographically-scanned elements of matrix E, $\Delta\boldsymbol{\alpha}$ is a vector of albedo changes at all locations (x,y) on the discretized floor grid, and C is a matrix of unit contributions whose rows correspond to (i,j) fixture-sensor pairs and columns correspond to locations (x,y).

Similarly to our previous method [37], we use a two-step approach to solve for $\Delta\boldsymbol{\alpha}$ with an important difference, which results in significantly improved localization accuracy. While they used a heuristic confidence map proposed by Wang *et al.* [31] as the first step, we take a principled approach based on ridge regression. In particular, we minimize the following cost function:

$$\min_{\Delta\boldsymbol{\alpha}_0} \left\|\mathbf{e} - \delta^2 C\Delta\boldsymbol{\alpha}_0\right\|_{l_2}^2 + \sigma\delta^2\|\Delta\boldsymbol{\alpha}_0\|_{l_2}^2 \tag{14}$$

where σ is a weight of the l_2 penalty term controlling the smoothness of the albedo change estimate. The optimal $\Delta\boldsymbol{\alpha}_0^*$ for (14) is a coarse estimate of the actual albedo change. We next threshold $|\Delta\boldsymbol{\alpha}_0^*|$ normalized by its maximum magnitude to obtain a set of locations

$$\mathcal{Q} = \left\{(x,y) : \frac{|\Delta\boldsymbol{\alpha}_0^*(x,y)|}{\max_{(x,y)}|\Delta\boldsymbol{\alpha}_0^*(x,y)|} \geq \tau\right\} \tag{15}$$

where the change in albedo is relatively large. These are likely to correspond to the area where the object appeared. Then, in the second step, we solve the ridge regression problem again, but the solution is now restricted to a subset of locations in $\mathcal{Q}$.

$$\begin{gathered}\min_{\Delta\boldsymbol{\alpha}} \left\|\mathbf{e} - \delta^2 C\Delta\boldsymbol{\alpha}\right\|_{l_2}^2 + \sigma\delta^2\|\Delta\boldsymbol{\alpha}\|_{l_2}^2 \\ \text{s.t. } \Delta\boldsymbol{\alpha}(x,y) = 0,\ \forall(x,y) \notin \mathcal{Q}\end{gathered} \tag{16}$$

Both minimizations (14) and (16) have a closed-form solution. After obtaining the optimal $\Delta\boldsymbol{\alpha}^*$ from (16), we use the centroid of the $|\Delta\boldsymbol{\alpha}^*|$ map as the estimated object location. The pseudo-code for this algorithm appears in Algorithm 2 below. Since σ and τ can affect the algorithm's performance, we use grid search to find the best set of parameters yielding the minimum average localization error.

Algorithm 2: Localization via Active Illumination

Input : Light transport matrices: A_0 for empty room and A for occupied room, room dimensions W, L and H, all light source and sensor coordinates

Output: Estimated location $(\widehat{x}_0, \widehat{y}_0)$

1 Calculate unit contribution matrix C where $C(i,j;x,y) = \text{const} \cdot \frac{q(\beta_j)\cos\beta_j\cos^2\theta_i}{D_j^2\cdot(H^2+l_i^2)}$ for $i \in \{1,\ldots,N_s\}$, $j \in \{1,\ldots,N_f\}$, $x \in [0,L]$, $y \in [0,W]$ with spacing δ;

2 Let $\mathbf{e}$ be the vector form of $E = A - A_0$;

3 Calculate the optimal solution $\Delta\boldsymbol{\alpha}_0^*$ for problem (14) without any constraint;

4 Threshold $|\Delta\boldsymbol{\alpha}_0^*|$ using τ to get the point set $\mathcal{Q}$;

5 Calculate the optimal solution $\Delta\boldsymbol{\alpha}^*$ for problem (16) with $\Delta\boldsymbol{\alpha}$ constrained inside $\mathcal{Q}$;

6 Estimated location: $(\widehat{x}_0, \widehat{y}_0) \leftarrow$ centroid of $|\Delta\boldsymbol{\alpha}^*|$.

3. Experimental Results

We have tested the performance of our localization algorithms in both simulated and real-world experiments. We performed simulations in `MATLAB` and Unity3D, a video game development environment. For our real-world experiments, we have built a small-scale testbed using a network of synchronized small LED light sources and single-pixel color sensors. We compare the performance of the proposed algorithms with our previous localized ridge regression algorithm [37] for 6 different object sizes. We also test our algorithms under illumination change between the empty and

occupied room states, and also in the presence of noise in sensor readings. Detailed information about our experimental setup, testbed, and results can be found on our project's web page [1].

3.1. Experiment Setup

In both the simulation and testbed experiments, the room has size W=122.5cm, L=223.8cm and H=70.5cm and 9 identical source-sensor modules are placed on the ceiling on a 3×3 grid (Fig. 3). Each module contains an LED light source and a single-pixel light sensor.

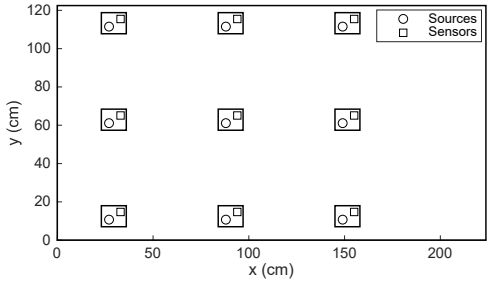

Figure 3. Layout of source-sensor modules on the ceiling.

We used flat (negligible height) rectangular objects of 6 different sizes (Table 1). Our object size choices are quite realistic at room-scale. For example, if we scale the testbed area 8 fold to a room of dimensions about 3.5×6m, then our smallest object (1x) will be about the size of a small plate (14cm diameter) and our largest object (64x) will be about the size of a table (70×140cm). We placed the objects on the floor so that their sides are parallel to those of the room.

Table 1. Dimensions of rectangular objects used in experiments.

Relative Size	Width (cm)	Length (cm)
64x	25.8	51.1
32x	25.8	25.5
16x	12.9	26.0
8x	12.9	13.0
4x	6.4	12.9
1x	3.2	6.4

In localization with active illumination, we obtained the light transport matrix A by following the steps detailed in Fig. 4. In localization with passive illumination, we turned on all 9 light sources to their maximum intensity and kept them unchanged. We kept the ambient light constant in all simulations and performed the testbed experiments at night with fluorescent lights as the only ambient light source.

3.2. Simulation Experiments

To validate our active and passive illumination algorithms, we simulated the room with light sources and sensors in both MATLAB and Unity3D, a game development environment that can simulate realistic scenes.

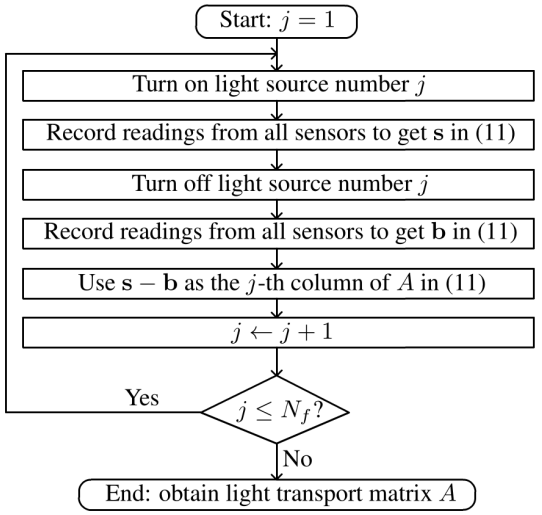

Figure 4. Steps followed to obtain the light transport matrix A.

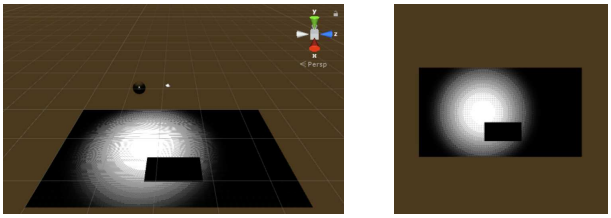

(a) Simulation of a light source with object placed on the floor

(b) Top view of the scene

Figure 5. Illustration of a Unity3D scene used in experiments.

In MATLAB simulation, we generated the floor albedo maps $\alpha(x, y)$ for empty and occupied states, and then calculated the sensor readings in each state using equations (1), (2) and (3). The MATLAB simulations are idealized since the sensor readings match the light reflection model perfectly with no inconsistencies.

To the best of our knowledge, Unity3D's built-in point light source does not allow different intensities in different directions. Therefore, to simulate a light source with a $q(\cdot)$ function, we placed the point light source at the center of a spherical cover. The cover is semi-transparent and blocks parts of the light from the source. We set the transparency of the cover at different angles differently in order to match the $q(\cdot)$ function. To simulate a light sensor, we placed Unity3D's virtual camera on the ceiling looking downward. The sensor reading is a weighted average of the camera's pixel values, where the weight is each pixel's solid angle to the center of the camera lens. To simulate sunlight (as part of ambient illumination), we used a directional light source which produces parallel rays. An illustration of a Unity3D scene of the room is shown in Fig. 5. The Unity3D model is only used to collect data while the localization algorithms are implemented in MATLAB.

In both MATLAB and Unity3D, we uniformly set the albedo of the floor to 0.5 and of the object to 0. We placed

the center of the object at 20 different locations equally-spaced on a 5×4 grid. We evaluated our algorithm's performance in terms of localization error defined as the Euclidean distance between the true and estimated locations. We compare the performance of our active and passive illumination algorithms with that of our previous algorithm [37]. The parameter σ of our previous algorithm and the set of parameters (σ, τ) of our active-illumination algorithm were chosen to minimize the average localization error using grid search.

First, we evaluated the performance of the three algorithms for different object sizes, in both simulation environments, without noise. The mean and standard deviation of the localization errors are shown in Table 2. We note that in MATLAB simulations, our new active illumination algorithm outperforms our previous algorithm [37] for all object sizes, and it performs better for larger objects. Our passive illumination algorithm works better for smaller objects, which is consistent with the negligible object size assumption (assumption 2 in Section 2.2) used to derive this algorithm. The Unity3D results exhibit a similar trend.

Fig. 6 shows an example of ground-truth location, albedo change map ($\Delta\boldsymbol{\alpha}$), and object locations estimated by our previous algorithm [37] and by the proposed active illumination algorithm, both simulated in MATLAB using a 64x object. The proposed algorithm performs better in estimating the object's location and the range of albedo change (as the object's albedo is lower than that of the background, $\Delta\alpha$ should be negative).

We also tested the robustness of both passive and active illumination algorithms under illumination change in Unity3D. An illumination change refers to the change of ambient light level $\mathbf{b}$ (11) between the empty and occupied room states. We performed tests using the 64x object, and turned on/off the simulated sun light to mimic day and night. The results are shown in Table 3. In the last two rows, when there is an illumination change, the performance of the passive illumination algorithm gets significantly worse, while the active illumination algorithm still performs well. This was to be expected since the passive illumination algorithm assumes that the only change in the sensor readings is caused by the object; it cannot handle illumination changes.

Furthermore, we tested the effect of sensor noise on the performance of our algorithms. We assumed that the noise corrupting each sensor reading is an independent and identically-distributed, zero-mean Gaussian. In MATLAB simulation, we added noise to all sensor readings in both the empty and occupied room states. We used the 16x object, and we varied the standard deviation of noise from 10^{-4} to

Table 2. Mean $\pm$ standard deviation of localization errors for three algorithms and each object size in MATLAB and Unity3D simulations with ambient illumination off. The smallest average localization errors are in bold.

	Object Size	Prev. work [37] (cm)	Passive (cm)	Active (cm)
MATLAB	64x	3.48 ± 1.91	3.52 ± 2.10	$\mathbf{0.04} \pm 0.04$
	32x	3.44 ± 1.80	0.85 ± 0.61	$\mathbf{0.06} \pm 0.07$
	16x	3.72 ± 2.84	0.97 ± 0.60	$\mathbf{0.16} \pm 0.10$
	8x	4.15 ± 2.78	0.23 ± 0.16	$\mathbf{0.22} \pm 0.13$
	4x	4.40 ± 3.03	$\mathbf{0.25} \pm 0.16$	0.40 ± 0.28
	1x	4.66 ± 3.30	$\mathbf{0.06} \pm 0.03$	0.58 ± 0.36
Unity3D	64x	3.98 ± 1.99	3.18 ± 1.74	$\mathbf{0.41} \pm 0.38$
	32x	6.09 ± 2.09	$\mathbf{0.28} \pm 0.17$	1.03 ± 0.81
	16x	6.24 ± 2.22	$\mathbf{0.93} \pm 0.61$	1.05 ± 0.72
	8x	6.15 ± 3.66	$\mathbf{0.66} \pm 0.52$	1.38 ± 1.12
	4x	6.22 ± 2.26	$\mathbf{0.40} \pm 0.33$	1.38 ± 1.10
	1x	6.62 ± 2.66	$\mathbf{0.51} \pm 0.45$	1.57 ± 1.18

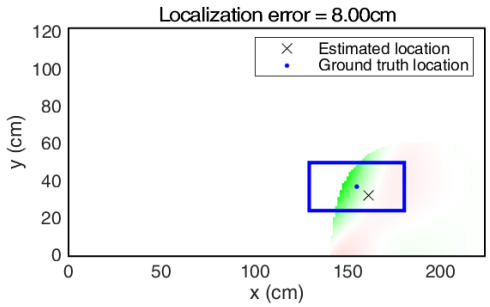

(a) Our previous algorithm [37]

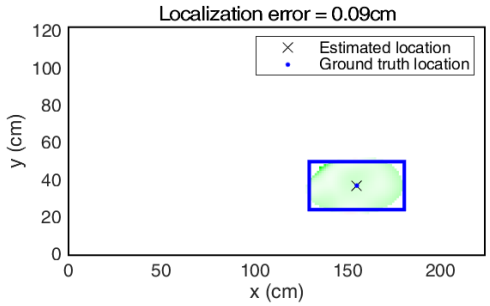

(b) Proposed algorithm

Figure 6. Example of ground-truth location, albedo change map and object location estimated by our previous algorithm [37] and the proposed active-illumination algorithm. The blue rectangle shows the boundary of the 64x object. Locations where $\Delta\alpha$ is positive are colored red and where $\Delta\alpha$ is negative are colored green.

Table 3. Mean $\pm$ standard deviation of localization errors for two proposed algorithms in Unity3D simulation with different ambient lighting combinations using the 64x object.

Ambient Lighting		Passive (cm)	Active (cm)
Empty Room	Occupied Room		
Day	Day	2.81 ± 1.33	0.41 ± 0.38
Night	Night	3.18 ± 1.74	0.41 ± 0.39
Day	Night	45.12 ± 19.72	0.38 ± 0.29
Night	Day	66.89 ± 28.26	0.46 ± 0.39

10^{-3} in 10^{-4} increments.[2] Fig. 7 shows the mean and standard deviation of localization errors for passive and active illumination algorithms as a function of the standard deviation of noise. Clearly, the passive illumination based localization error is almost an order of magnitude larger than the error for active illumination.

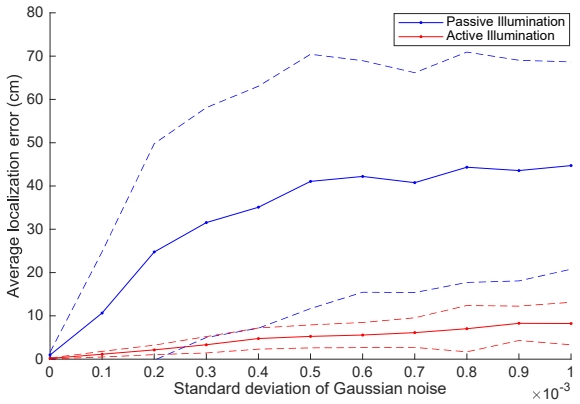

Figure 7. Localization error for the proposed algorithms with respect to the standard deviation of Gaussian noise. The solid lines show mean localization errors, while the dashed lines correspond to error bars indicating the standard deviation of errors. Each value is calculated by combining results from 3 repetitions of the experiment. For each noise level, the parameters σ and τ for the active illumination algorithm are optimized with grid search using a separate set of measurements.

3.3. Testbed Experiments

To test our approach in a real-world setting, we built a room mock-up using a white rectangular foam board as the floor and a 3×3 array of ceiling-mounted light source-sensor modules. Each module consists of a Particle Photon board controlling an LED and a single-pixel light sensor. We estimated the $q(\cdot)$ function (Fig. 2) by averaging several measurements of our LEDs. We note that the sensors have no lens and measure photon flux not radiance. This is a small-scale proof-of-concept testbed to quantitatively validate the feasibility of active-illumination based indoor localization. Although idealized (no walls/furniture, floor and objects have uniform albedo), it is a much-needed first step before developing a full-scale smart-room testbed. While this is not an accurate representation of complex real-world scenarios, it does capture real-world non-idealities such as sensor noise, non-Lambertian surfaces, indirect light, and fluorescent light flicker and provides insights into the localization accuracy relative to testbed dimensions.

During data collection, the LEDs turn on all 4 channels (red, green, blue and white) at maximum intensity in a preset order and the single-pixel sensors record readings from the white channel only (red, green and blue channel readings are ignored). When a sensor records, it takes 4 consecutive readings which are then averaged together to reduce noise. This process yields 81 noise-reduced sensor readings in the active illumination data collection processes, and, respectively, 9 readings in the passive illumination case.

[2] 10^{-3} represents about 6.84% of the maximum change in any sensor's reading between empty and occupied room states.

Table 4. Mean $\pm$ standard deviation of localization errors for three algorithms and four object sizes in the real testbed with fluorescent light off. The smallest average localization errors are in bold.

Object Size	Previous work [37] (cm)	Passive (cm)	Active (cm)
64x	7.80 ± 5.11	49.19 ± 26.88	$\mathbf{3.40} \pm 1.56$
32x	10.16 ± 5.68	47.91 ± 24.34	$\mathbf{4.13} \pm 2.48$
16x	11.29 ± 5.49	49.79 ± 23.13	$\mathbf{4.41} \pm 2.50$
8x	27.75 ± 27.22	56.23 ± 22.45	$\mathbf{5.99} \pm 3.93$

Table 5. Mean $\pm$ standard deviation of localization errors of the proposed algorithms in MATLAB simulation with Gaussian noise added to match testbed conditions. Results are for the 16x object and are based on 3 simulation runs.

Simulation run	Passive (cm)	Active (cm)
1	54.02 ± 22.43	6.61 ± 4.24
2	53.83 ± 21.92	5.33 ± 3.17
3	49.96 ± 24.55	5.71 ± 2.54

Similarly to the simulation experiments, we compare the performance of the algorithms in the testbed for different object sizes (from 8x to 64x) at all 20 locations. We did not use the 1x and 4x objects because their sensor reading changes are too small and get buried in noise. We recorded data in a completely dark room with no ambient illumination (fluorescent lights off).

As shown in Table 4, our new active-illumination algorithm outperforms our previous algorithm [37] in the testbed. However, our passive illumination algorithm has poor performance compared to both active illumination algorithms. As Fig. 7 suggests, this is likely due to the higher sensitivity of the passive illumination algorithm to sensor noise. In order to verify this hypothesis, we first measured the standard deviation of the readings of each sensor from the testbed data. We then added Gaussian noise (having the same relative standard deviations as in the testbed) to the readings of the corresponding sensors in the MATLAB simulation. The localization errors are shown in Table 5. We see that the performance of passive and active illumination algorithms in MATLAB simulation under noise is similar to their performance in the testbed. This suggests that noise is the main reason why passive illumination performs poorly.

Finally, we tested the robustness of both algorithms under illumination change for the 64x object. We applied different ambient lighting combinations for the empty and occupied room states (fluorescent lights on or off). As can be seen in Table 6, the performance of the active illumination algorithm remains good under illumination change, which

Table 6. Mean ± standard deviation of localization errors for the proposed algorithms with different ambient lighting combinations in the testbed (64x object). "Bright" or "Dark" means the fluorescent light is on or off, respectively.

Ambient Lighting		Passive (cm)	Active (cm)
Empty Room	Occupied Room		
Bright	Bright	42.43 ± 25.38	8.19 ± 7.29
Dark	Dark	49.19 ± 26.88	3.40 ± 1.56
Bright	Dark	54.76 ± 19.76	4.21 ± 2.30
Dark	Bright	61.92 ± 21.55	7.36 ± 7.49

is consistent with the simulations. The passive illumination algorithm, however, performs only slightly worse than without illumination changes. This is not unexpected since its performance without illumination changes was already poor (Table 4).

4. Discussion

4.1. Effect of Object Size

In both simulated and real-testbed experiments, our active illumination based localization algorithm outperforms our previous algorithm [37] for all object sizes (Tables 2 and 4). The new active illumination algorithm performs better for larger objects but slightly worse for smaller ones. This is because the l_2 penalty term in the cost function smooths the $\Delta\alpha$ map and therefore favors large objects. On the contrary, the passive illumination algorithm performs better for smaller objects in the simulation because the algorithm assumes that the object size is negligible compared to the floor size. Also, we note that the passive illumination algorithm outperforms the active illumination algorithm for small objects like 4x and 1x in MATLAB, and for all objects except the 64x one in Unity3D. Ideally, active illumination based localization should have smaller error than passive illumination based localization for all object sizes since it has more information. This suggests that our active illumination algorithm is sub-optimal and is not making the best use of all the information available to it. It could potentially be improved and this is part of our ongoing work.

4.2. Effect of Illumination Change

The experimental results in Tables 3 and 6 suggest that the active illumination algorithm is robust under illumination change while the passive illumination algorithm is not. This is consistent with the assumptions used to derive each algorithm. The passive illumination algorithm assumes that the change in the sensor reading is only due to the arrival of an object and does not account for the possibility of illumination change between the empty and occupied room states. The active illumination algorithm, however, only needs to compute the change in the light transport matrix between the empty and occupied room states. The light transport matrix is determined by room geometry, sensor and source placements and floor albedo distribution, and is unaffected by ambient light. The estimation of a light transport matrix too is unaffected by ambient light since it is based on measuring the *change* in sensor readings due to light modulation. The only crucial assumption needed for this to succeed is that the ambient light remains constant during the process of measuring a single light transport matrix. This is easily ensured by the short modulation-response time.

4.3. Effect of Noise

The results in Fig. 7 and Table 5 suggest that the passive-illumination algorithm is more sensitive to noise than the active-illumination algorithm. In passive illumination, equation (6) is based on the ratio of changes in the sensor readings. The sensor reading changes can be small, depending on the object size and location; taking a ratio of changes can magnify the error. In active illumination, the parameter σ can be adjusted to adapt to noise. We observed in our MATLAB simulations that the best σ is larger when the noise standard deviation is larger. By adding more weight to the l_2 penalty term, the active illumination algorithm makes the optimal $\Delta\boldsymbol{\alpha}^*$ smoother and adapts to a higher level of noise.

4.4. Privacy Preservation

By replacing high-resolution cameras with single-pixel color sensors, our indoor localization system preserves the visual privacy of occupants while providing utility (location information). Qualitatively, the albedo change map (Fig. 6) does not appear to have enough information to reliably estimate object shape, size, color, or texture. This needs to be quantified and is part of our future work.

5. Conclusions and Outlook

A key message of this work is that active illumination based indoor localization provides a number of benefits including visual privacy, smaller localization error, and robustness to noise and illumination changes. This was demonstrated *via* simulations and a small-scale proof-of-concept testbed that captured, to a limited extent, certain real-world complexities such as non-Lambertian surfaces, indirect light, and fluorescent light flicker. Our study focused on a single, static, flat rectangular object, but our approach can be extended to well-separated multiple slowly-moving objects using background subtraction applied to light transport matrices. Also, in our ongoing work, we plan to expand our testbed to room scale and generalize our algorithmic framework to handle complex three dimensional objects. As an alternative to model-based methods that we have explored here, we are also investigating adaptive data-driven methods for both passive and active illumination which do not require prior knowledge of the room geometry, source/sensor locations, and their characteristics.

References

[1] Privacy-preserving localization via active scene illumination. http://vip.bu.edu/projects/vsns/privacy-smartroom/active-illumination/. Last accessed: April 15, 2018. 5

[2] Ambiplex. http://www.ambiplex.com/, 2011. Last accessed: November 29, 2017. 1

[3] S. Afshari, T.-K. Woodstock, M. Imam, S. Mishra, A. C. Sanderson, and R. J. Radke. Short paper:: The smart conference room: an integrated system testbed for efficient, occupancy-aware lighting control. In *Proceedings of the 2nd ACM International Conference on Embedded Systems for Energy-Efficient Built Environments*, pages 245–248. ACM, 2015. 1

[4] I. Bhattacharya and R. J. Radke. Arrays of single pixel time-of-flight sensors for privacy preserving tracking and coarse pose estimation. In *Applications of Computer Vision (WACV), 2016 IEEE Winter Conference on*, pages 1–9. IEEE, 2016. 1

[5] K. Brkic, I. Sikiric, T. Hrkac, and Z. Kalafatic. I know that person: Generative full body and face de-identification of people in images. *CVPRW*, 1(2):4, 2017. 1

[6] B. Brumitt, B. Meyers, J. Krumm, A. Kern, and S. Shafer. Easyliving: Technologies for intelligent environments. In *International Symposium on Handheld and Ubiquitous Computing*, pages 12–29. Springer, 2000. 1

[7] J. Chen, J. Wu, K. Richter, J. Konrad, and P. Ishwar. Estimating head pose orientation using extremely low resolution images. In *Image Analysis and Interpretation (SSIAI), 2016 IEEE Southwest Symposium on*, pages 65–68. IEEE, 2016. 1

[8] J. Dai, J. Wu, B. Saghafi, J. Konrad, and P. Ishwar. Towards privacy-preserving activity recognition using extremely low temporal and spatial resolution cameras. In *Proceedings of the IEEE Conference on Computer Vision and Pattern Recognition Workshops*, pages 68–76, 2015. 1

[9] A. Erdélyi, T. Barát, P. Valet, T. Winkler, and B. Rinner. Adaptive cartooning for privacy protection in camera networks. In *Advanced Video and Signal Based Surveillance (AVSS), 2014 11th IEEE International Conference on*, pages 44–49. IEEE, 2014. 1

[10] L. M. Frazier. Surveillance through walls and other opaque materials. In *Radar Conference, 1996., Proceedings of the 1996 IEEE National*, pages 27–31. IEEE, 1996. 1

[11] X. Guo, D. Tiller, G. Henze, and C. Waters. The performance of occupancy-based lighting control systems: A review. *Lighting Research & Technology*, 42(4):415–431, 2010. 1

[12] E. T. Hassan, R. Hasan, P. Shaffer, D. Crandall, and A. Kapadia. Cartooning for enhanced privacy in lifelogging and streaming videos. *CVPRW*, 1:4, 2017. 1

[13] D. Hauschildt and N. Kirchhof. Advances in thermal infrared localization: Challenges and solutions. In *Indoor Positioning and Indoor Navigation (IPIN), 2010 International Conference on*, pages 1–8. IEEE, 2010. 1

[14] J. Hightower, R. Want, and G. Borriello. Spoton: An indoor 3d location sensing technology based on rf signal strength. *UW CSE 00-02-02, University of Washington, Department of Computer Science and Engineering, Seattle, WA*, 1, 2000. 1

[15] Q. Huang, Z. Ge, and C. Lu. Occupancy estimation in smart buildings using audio-processing techniques. *arXiv preprint arXiv:1602.08507*, 2016. 1

[16] L. Jia and R. J. Radke. Using time-of-flight measurements for privacy-preserving tracking in a smart room. *IEEE Transactions on Industrial Informatics*, 10(1):689–696, 2014. 1

[17] T. K. Kohoutek, R. Mautz, and A. Donaubauer. Real-time indoor positioning using range imaging sensors. In *Real-Time Image and Video Processing 2010*, volume 7724, page 77240K. International Society for Optics and Photonics, 2010. 1

[18] A. E. Kosba, A. Abdelkader, and M. Youssef. Analysis of a device-free passive tracking system in typical wireless environments. In *New Technologies, Mobility and Security (NTMS), 2009 3rd International Conference on*, pages 1–5. IEEE, 2009. 1

[19] J. Krumm. *Ubiquitous computing fundamentals*. CRC Press, 2016. 1

[20] K. Kunze and P. Lukowicz. Sensor placement variations in wearable activity recognition. *IEEE Pervasive Computing*, 13(4):32–41, 2014. 1

[21] L. Ma, Z. Zhang, and X. Tan. A novel through-wall imaging method using ultra wideband pulse system. In *Intelligent Information Hiding and Multimedia Signal Processing, 2006. IIH-MSP'06. International Conference on*, pages 147–150. IEEE, 2006. 1

[22] M. Moussa and M. Youssef. Smart cevices for smart environments: Device-free passive detection in real environments. In *Pervasive Computing and Communications, 2009. PerCom 2009. IEEE International Conference on*, pages 1–6. IEEE, 2009. 1

[23] R. Munoz-Salinas, R. Medina-Carnicer, F. J. Madrid-Cuevas, and A. Carmona-Poyato. Multi-camera people tracking using evidential filters. *International Journal of Approximate Reasoning*, 50(5):732–749, 2009. 1

[24] L. M. Ni, Y. Liu, Y. C. Lau, and A. P. Patil. Landmarc: indoor location sensing using active rfid. *Wireless networks*, 10(6):701–710, 2004. 1

[25] V. A. Petrushin, G. Wei, and A. V. Gershman. Multiple-camera people localization in an indoor environment. *Knowledge and Information Systems*, 10(2):229–241, 2006. 1

[26] N. B. Priyantha, A. Chakraborty, and H. Balakrishnan. The cricket location-support system. In *Proceedings of the 6th annual international conference on Mobile computing and networking*, pages 32–43. ACM, 2000. 1

[27] N. Raval, A. Machanavajjhala, and L. P. Cox. Protecting visual secrets using adversarial nets. In *Computer Vision and Pattern Recognition Workshops (CVPRW), 2017 IEEE Conference on*, pages 1329–1332. IEEE, 2017. 1

[28] J. Reijniers and H. Peremans. Biomimetic sonar system performing spectrum-based localization. *IEEE Transactions on Robotics*, 23(6):1151–1159, 2007. 1

[29] D. Roeper, J. Chen, J. Konrad, and P. Ishwar. Privacy-preserving, indoor occupant localization using a network of

single-pixel sensors. In *Proc. IEEE Int. Conf. Advanced Video and Signal-Based Surveillance*, Aug. 2016. 1

[30] E. A. Wan and A. S. Paul. A tag-free solution to unobtrusive indoor tracking using wall-mounted ultrasonic transducers. In *Indoor Positioning and Indoor Navigation (IPIN), 2010 International Conference on*, pages 1–10. IEEE, 2010. 1

[31] Q. Wang, X. Zhang, and K. L. Boyer. Occupancy distribution estimation for smart light delivery with perturbation-modulated light sensing. *Journal of solid state lighting*, 1(1):17, 2014. 1, 2, 4

[32] X. Wang and S. Wang. Collaborative signal processing for target tracking in distributed wireless sensor networks. *Journal of Parallel and Distributed Computing*, 67(5):501–515, 2007. 1

[33] R. Want, A. Hopper, V. Falcao, and J. Gibbons. The active badge location system. *ACM Transactions on Information Systems (TOIS)*, 10(1):91–102, 1992. 1

[34] J. Wilson and N. Patwari. Through-wall tracking using variance-based radio tomography networks. *arXiv preprint arXiv:0909.5417*, 2009. 1

[35] M. Youssef, M. Mah, and A. Agrawala. Challenges: device-free passive localization for wireless environments. In *Proceedings of the 13th annual ACM international conference on Mobile computing and networking*, pages 222–229. ACM, 2007. 1

[36] W. Zajdel and B. J. Kröse. A sequential bayesian algorithm for surveillance with nonoverlapping cameras. *International Journal of Pattern Recognition and Artificial Intelligence*, 19(08):977–996, 2005. 1

[37] J. Zhao, P. Ishwar, and J. Konrad. Privacy-preserving indoor localization via light transport analysis. In *Acoustics, Speech and Signal Processing (ICASSP), 2017 IEEE International Conference on*, pages 3331–3335. IEEE, 2017. 2, 4, 6, 7, 8